



Contents lists available at ScienceDirect

## European Journal of Medicinal Chemistry

journal homepage: <http://www.elsevier.com/locate/ejmech>

Short communication

PET radiotracer [ $^{18}\text{F}$ ]-P6 selectively targeting COX-1 as a novel biomarker in ovarian cancer: Preliminary investigation

Maria Grazia Perrone<sup>a,1</sup>, Paola Malerba<sup>a,1</sup>, Md. Jashim Uddin<sup>b</sup>, Paola Vitale<sup>a</sup>,  
 Andrea Panella<sup>a</sup>, Brenda C. Crews<sup>b</sup>, Cristina K. Daniel<sup>b</sup>, Kebreab Ghebreselasie<sup>b</sup>,  
 Mike Nickels<sup>c</sup>, Mohammed N. Tantawy<sup>c</sup>, H. Charles Manning<sup>c</sup>, Lawrence J. Marnett<sup>b,\*</sup>,  
 Antonio Scilimati<sup>a,\*</sup>

<sup>a</sup> Dipartimento di Farmacia-Scienze del Farmaco, Università degli Studi di Bari "A. Moro", Via E. Orabona 4, 70125 Bari, Italy<sup>b</sup> A.B. Hancock, Jr., Memorial Laboratory for Cancer Research, Department of Biochemistry, Chemistry and Pharmacology, Vanderbilt Institute of Chemical Biology, Nashville, TN 37232-0146, USA<sup>c</sup> Department of Radiology and Radiological Sciences, Vanderbilt Institute of Imaging Sciences, Vanderbilt University School of Medicine, Nashville, TN 37232-0146, USA

## ARTICLE INFO

## Article history:

Received 30 September 2013

Received in revised form

23 April 2014

Accepted 25 April 2014

Available online 29 April 2014

## Keywords:

[ $^{18}\text{F}$ ]-P6 radiotracer

Cyclooxygenase (COX)-1

Ovarian cancer

Biomarker

OVCAR-3 cell

PET-CT imaging

## ABSTRACT

Cyclooxygenase-1 (COX-1), but not COX-2, is expressed at high levels in the early stages of human epithelial ovarian cancer where it seems to play a key role in cancer onset and progression. As a consequence, COX-1 is an ideal biomarker for early ovarian cancer detection. A series of novel fluorinated COX-1-targeted imaging agents derived from P6 was developed by using a highly selective COX-1 inhibitor as a lead compound. Among these new compounds, designed by structural modification of P6, 3-(5-chlorofuran-2-yl)-5-(fluoromethyl)-4-phenylisoxazole ([ $^{18}\text{F}$ ]-P6) is the most promising derivative [ $\text{IC}_{50}$  = 2.0  $\mu\text{M}$  (purified oCOX-1) and 1.37  $\mu\text{M}$  (hOVCAR-3 cell COX-1)]. Its tosylate precursor was also prepared and, a method for radio[ $^{18}\text{F}$ ]chemistry was developed and optimized. The radiochemistry was carried out using a carrier-free  $\text{K}^{18}\text{F}$ /Kryptofix 2.2.2 complex, that afforded [ $^{18}\text{F}$ ]-P6 in good radiochemical yield (18%) and high purity (>95%). *In vivo* PET/CT imaging data showed that the radiotracer [ $^{18}\text{F}$ ]-P6 was selectively taken up by COX-1-expressing ovarian carcinoma (OVCAR 3) tumor xenografts as compared with the normal leg muscle. Our results suggest that [ $^{18}\text{F}$ ]-P6 might be an useful radiotracer in preclinical and clinical settings for *in vivo* PET-CT imaging of tissues that express elevated levels of COX-1.

© 2014 Elsevier Masson SAS. All rights reserved.

## 1. Introduction

Cyclooxygenases (COX-1 and COX-2) catalyze the biotransformation of arachidonic acid into prostanoids [1,2]. The constitutively expressed isoform COX-1 is responsible for maintaining homeostasis (gastric and renal integrity) and normal production of eicosanoids [3], whereas the inducible isoform COX-2 is implicated in the synthesis of prostanoids involved in acute and chronic inflammatory processes. In addition to its role in inflammatory disorders, COX-2 has an important function in carcinogenesis by stimulating angiogenesis, tissue invasion, metastasis, and apoptosis inhibition [4]. Recent reports have proven the COX-1 role in several

human pathologies, including neuroinflammation [5,6] (as the earliest stage of some neurodegenerative diseases such as Alzheimer- and Parkinson-disease), atherosclerosis [7], endothelial dysfunction [8], preterm labor [9], pain [10], and carcinogenesis [11–15]. In particular, COX-1 is overexpressed in various stages (onset and progression) of human epithelial ovarian cancers, where it controls the production of prostaglandins and promotes angiogenic growth factor production [13,16,17]. Moreover, in an *in vivo* model obtained with ovarian surface epithelial (OSE) cells allografted in female nude mice, SC-560 [18], a highly selective COX-1 inhibitor, significantly reduces the tumor growth [19]. On the other hand, celecoxib, a selective COX-2 inhibitor, has no significant effect, suggesting that, COX-1 is the primary player for the generation of prostaglandins in murine epithelial ovarian cancers (EOCs) [16]. Similar studies, accomplished by treating mice bearing human ovarian SKOV-3 carcinoma xenografts, have shown that SC-560, used alone or in combination with the non selective COX inhibitor

\* Corresponding authors.

E-mail addresses: [larry.marnett@vanderbilt.edu](mailto:larry.marnett@vanderbilt.edu) (L.J. Marnett), [antonio.scilimati@uniba.it](mailto:antonio.scilimati@uniba.it) (A. Scilimati).<sup>1</sup> These authors equally contributed to the project.

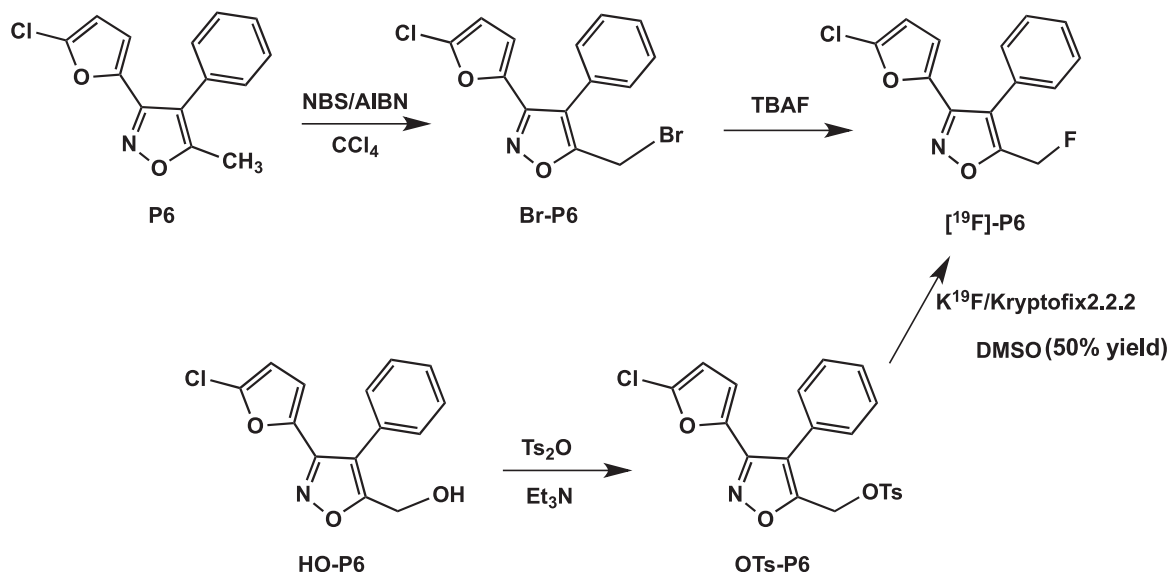
ibuprofen, significantly reduces tumor growth and angiogenesis [19,20]. As a consequence, COX-1 might be an ideal target for theranostic investigations of human epithelial ovarian cancers. Unfortunately, treatment of these neoplastic diseases is still limited [20] because of the lack of a non-invasive and effective imaging agent for early diagnosis. So, development of a COX-1-targeted Positron Emission Tomography (PET) radiotracer is a matter of extreme importance.

As a continuation of our previous investigations [21–24], herein we report the synthesis, the biochemical and cellular evaluation of a **P6** [3-(5-chlorofuran-2-yl)-5-methyl-4-phenylisoxazole] [21] derived [ $^{18}\text{F}$ ]-fluorinated COX-1 inhibitor, as a COX-1-targeted PET imaging agent. In addition, we describe the radiochemical synthesis of the promising compound [ $^{18}\text{F}$ ]-**P6** and its *in vivo* delivery into human OVCAR-3 (ovarian cancer) tumor xenografts expressing elevated levels of COX-1.

## 2. Results and discussion

We designed fluorinated COX-1-targeted PET imaging agents based on the chemical structure of **P6**, a highly selective COX-1 inhibitor (COX-1  $\text{IC}_{50} = 0.5 \mu\text{M}$ , COX-2  $\text{IC}_{50} > 100 \mu\text{M}$ , measured by human whole blood assay) [21,25], and identified a novel fluorinated-**P6** as a potent and selective COX-1 inhibitor. A *one-pot* procedure towards the isoxazole scaffold, involves the reaction of aryl nitrile oxides and the enolates of 3-aryl-2-propanones [23–26]. In particular, 3-(5-chlorofuran-2-yl)-5-(fluoromethyl)-4-phenylisoxazole ( $^{19}\text{F}$ )-**P6** was prepared starting from **P6**, first converted into 5-bromomethyl-3-(5-chlorofuran-2-yl)-4-phenylisoxazole (**Br-P6**) by bromination with *N*-bromosuccinimide (NBS) in the presence of azobisisobutyronitrile (AIBN) as a radical initiator. Then, **Br-P6** reacted with anhydrous tetrabutylammonium fluoride (TBAF) to afford the target [ $^{19}\text{F}$ ]-**P6**. The latter was also prepared starting from the alcohol **HO-P6** [23,25] previously transformed into its tosylate **OTs-P6** by reaction with  $\text{Ts}_2\text{O}$  in the presence of  $\text{Et}_3\text{N}$ . The tosylate derivative was then treated with  $\text{K}^{19}\text{F}$ /Kryptofix for the radiomimetic approach (Scheme 1).

The  $\text{IC}_{50}$  values for inhibition of purified *m*COX-2 and *o*COX-1 enzymes by [ $^{19}\text{F}$ ]-**P6** were determined by a thin layer chromatography (TLC) assay (Fig. 1a) [27].



**Scheme 1.** Synthesis of 3-(5-chlorofuran-2-yl)-5-(fluoromethyl)-4-phenylisoxazole, [ $^{19}\text{F}$ ]-**P6**. NBS = *N*-bromosuccinimide; AIBN = 2,2'-Azobis(2-methylpropionitrile); TBAF = Tetrabutylammonium fluoride;  $\text{Ts}_2\text{O}$  = *p*-Toluenesulfonic anhydride;  $\text{Et}_3\text{N}$  = Triethylamine.

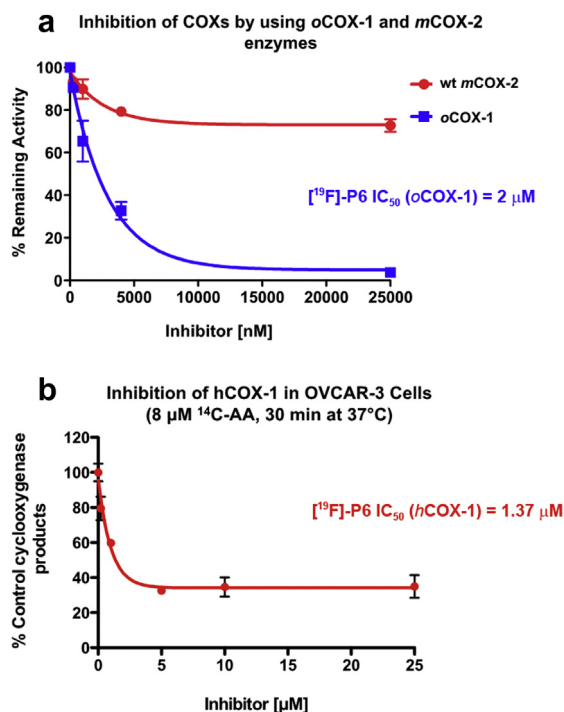


**Fig. 1.** [ $^{19}\text{F}$ ]-**P6**  $\text{IC}_{50}$  values determination: (a) inhibition of *in vitro* purified *o*COX-1 and *m*COX-2; (b) inhibition assay of OVCAR-3 intracellular *h*COX-1 performed in the presence of  $8 \mu\text{M}$  [ $^{14}\text{C}$ ]-AA and increasing amount of [ $^{19}\text{F}$ ]-**P6**.

Hematin-reconstituted murine COX-2 (66 nM) or ovine COX-1 (44 nM) in 100 mM Tris-HCl, pH 8.0 containing 500  $\mu\text{M}$  phenol was treated with several concentrations of inhibitor (0–66  $\mu\text{M}$ ) at  $25^\circ\text{C}$  for 17 min and  $37^\circ\text{C}$  for 3 min followed by metabolism of [ $^{14}\text{C}$ ]-arachidonic acid (50  $\mu\text{M}$ ) for 30 s at  $37^\circ\text{C}$ . In this assay, [ $^{19}\text{F}$ ]-**P6** showed selective COX-1 inhibitory activity.

The ability of the promising fluorinated **P6** analogue to inhibit COX-1 activity in intact cells was also evaluated by using the human ovarian cancer cell line OVCAR-3 (Fig. 1b) [13,16,28], in which high levels of COX-1 expression and no detectable COX-2 were found by

Western Blotting Assay [16]. [ $^{19}\text{F}$ ]-P6, incubated with OVCAR-3 cells in the presence of [ $^{14}\text{C}$ ]-arachidonic acid, significantly reduced intracellular COX-1-mediated AA metabolism ( $h\text{COX-1}$   $\text{IC}_{50} = 1.37 \mu\text{M}$ ).

Furthermore, [ $^{19}\text{F}$ ]-P6 up to  $100 \mu\text{M}$  did not affect at all the OVCAR-3 cell viability within 48 h.

The radiosynthesis of [ $^{18}\text{F}$ ]-P6 was accomplished, on a commercially available GE Tracerlab  $\text{FX}_{\text{FN}}$  automated reaction module, by a  $^{18}\text{F}$ -nucleophilic substitution on the tosylate precursor (OTs-P6) performed in the presence of  $\text{K}^{18}\text{F}$ /Kryptofix 2.2.2 (Scheme 2).

This reaction was preceded by a radiomimetic synthesis of [ $^{19}\text{F}$ ]-P6 in which it was obtained in 50% yield (Scheme 1).

Then, the ability of [ $^{18}\text{F}$ ]-P6 to target COX-1 in human ovarian tumor xenografts in female nude mice was evaluated. The novel radiotracer was administered by intra-peritoneal injection, then the mice were sacrificed by isoflurane overdose. The OVCAR-3 tumors were removed and weighed, and the radioactivity associated with each tumor was counted with a well gamma counter. After normalization of uptake (Bq/g), the OVCAR-3 tumors showed approximately an 8-fold higher uptake of the radiotracer compared with normal leg muscle (Fig. 2,  $n = 3$ ,  $p = 0.01$ ), thus suggesting a selective uptake of the positron emitting agent [ $^{18}\text{F}$ ]-P6 in the tumor expressing COX-1-targeted due to the presence of COX-1 protein in OVCAR-3 cell induced-tumor.

Moreover, the PET and CT images were co-registered to each other on the basis of bed position and even though [ $^{18}\text{F}$ ]-P6 radiotracer uptake in the OVCAR 3-induced tumors was 0.35% of the injected dose/g, PET imaging did not show a marked selective uptake. The different results might be due to the lower *in vivo* PET detector sensitivity than that of Geiger counter in measuring tissue extract radioactivity (Fig. 3). This would also indicate that not enough material has been delivered to the tumor and that greater radiotracer amount or more potent COX-1 inhibitors are needed. Further and deeper studies (dynamic PET imaging recordings) are ongoing.

*In vivo* stability of compound [ $^{19}\text{F}$ ]-P6 was evaluated by analyzing the tissue samples on an LC-ESI-MS system. The nude mice bearing OVCAR-3 xenografts were dosed with intraperitoneal (i.p.) injection of [ $^{19}\text{F}$ ]-P6. The intact parent compound [ $^{19}\text{F}$ ]-P6 was identified in the tumors on an average of  $63 \text{ pmol/g}$  tissue ( $n = 4$ ) (Fig. 4). A minimal or no amount of the compound [ $^{19}\text{F}$ ]-P6 was detected in the normal leg muscles. Also, no defluorinated metabolite (compound HO-P6) was detected in any of the tissue samples analyzed, suggesting that compound [ $^{19}\text{F}$ ]-P6 remained intact in the biological environment for long enough period of time to be taken up by the COX-1-expressing tumors (Fig. 4).

### 3. Conclusions

A novel compound [ $^{18}\text{F}$ ]-P6 was identified as a promising lead for a COX-1-targeted PET imaging agent. The synthetic procedure to prepare [ $^{19}\text{F}$ ]-P6, and OTs-P6 for the incorporation

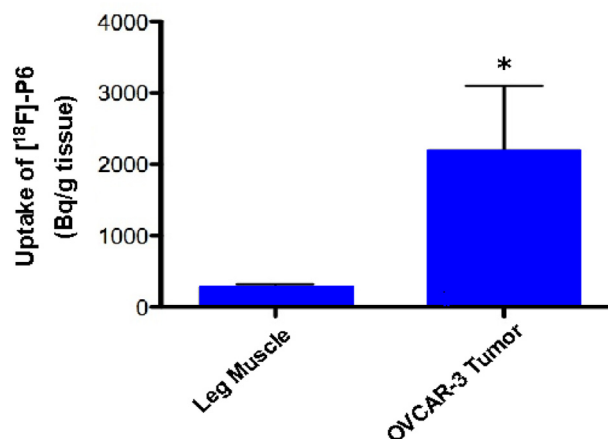


Fig. 2. *In vivo* uptake in tumors. Female nude mice bearing OVCAR-3 xenografts were dosed with compound [ $^{18}\text{F}$ ]-P6 (7.4 MBq, intraperitoneal injection). Then, the animals were sacrificed by isoflurane overdose. The OVCAR-3 tumor and normal leg muscles were removed and weighed, and radioactivity associated with each tissue was counted in a well gamma counter. The plot shows the increased radiotracer (Bq/g) in COX-1-expressing OVCAR-3 tumors versus normal leg muscle ( $n = 3$ ,  $p = 0.01$ ) (\*statistical significance).

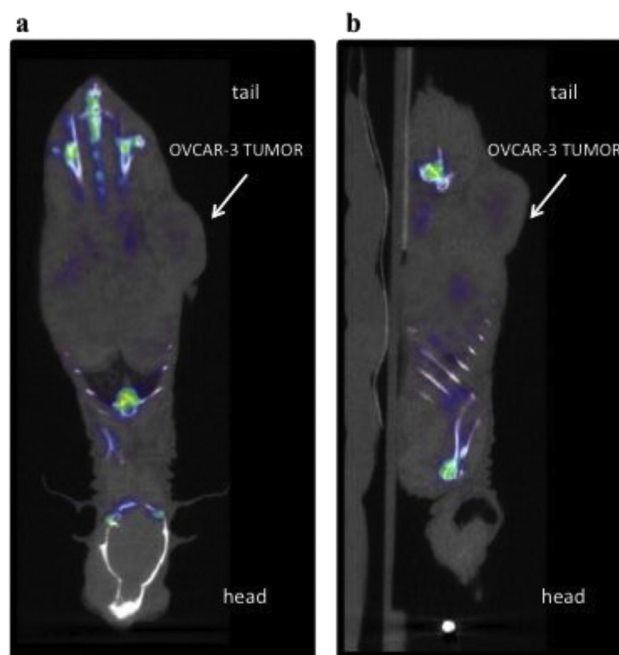
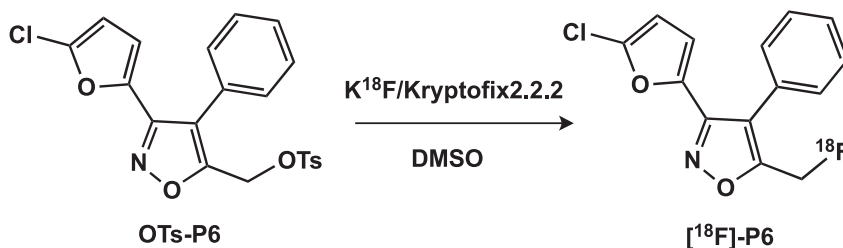
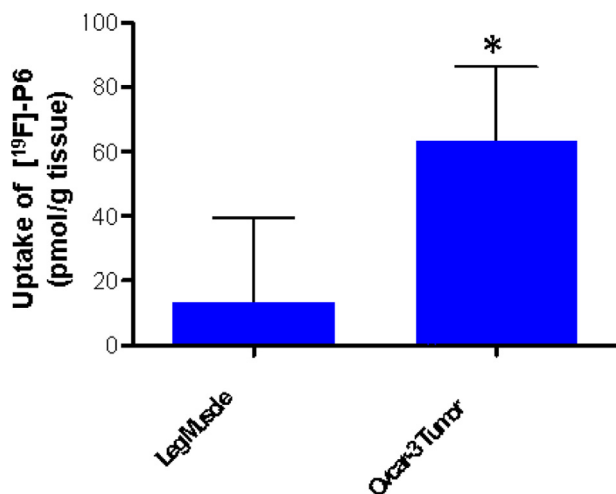


Fig. 3. *In vivo* PET imaging of COX-1-expressing tumor by [ $^{18}\text{F}$ ]-P6. (a) Coronal view, (b) Sagittal view. Tumor-bearing female nude mice were dosed by i.p. injection with compound [ $^{18}\text{F}$ ]-P6 ( $100 \mu\text{L}$ , 7.4 MBq, intraperitoneal injection) under anesthesia. At 4 h post injection, the animals were imaged in the microPET/CT instrument (30-min acquisition).



Scheme 2. Radiosynthesis of [ $^{18}\text{F}$ ]-P6. DMSO = dimethylsulfoxide.



**Fig. 4.** OVCAR-3 tumor and normal leg muscles were removed and amount of compound [<sup>19</sup>F]-P6 was determined by LC-MS. The plot shows the increased unlabeled compound [<sup>19</sup>F]-P6 in COX-1-expressing OVCAR-3 tumors versus normal leg muscle ( $n = 4$ ,  $p = 0.01$ ) (\*statistical significance).

of fluorine-18 to obtain the radiolabeled [<sup>18</sup>F]-P6 was optimized. [<sup>19</sup>F]-P6 showed a high degree of selectivity towards *in vitro* and *in vivo* COX-1 inhibition and uptake into OVCAR-3 xenografts in immuno-compromised mice. Its  $IC_{50}$  is 1.37  $\mu$ M in OVCAR-3 cells and 2  $\mu$ M and >100  $\mu$ M in purified oCOX-1 and mCOX-2 enzymes, respectively. A suitable *in vivo* stability of [<sup>19</sup>F]-P6 was found in tumor, moreover no defluorinated derivative was detected in any analyzed tissue. These preliminary results indicate that [<sup>18</sup>F]-P6, a fluorinated COX-1 selective inhibitor, might be a good radiotracer to detect early stages of EOCs, further experiments are ongoing to provide more evidences to certificate [<sup>18</sup>F]-P6 as a tracer in EOCs.

## 4. Experimental protocols

### 4.1. General

Melting points taken on Electrothermal apparatus were uncorrected. <sup>1</sup>H NMR and <sup>13</sup>C NMR spectra were recorded on a Varian-Mercury 300 MHz, Varian-Inova-400 MHz spectrometer, Bruker-Aspect 3000 console-500 MHz spectrometer, Bruker AV-I console operating at 400.13 MHz, or a Bruker DRX console operating at 600.13 MHz. Chemical shifts are reported in parts per million ( $\delta$ ). Fluorine spectra were recorded by using CFCl<sub>3</sub> as internal standard. Absolute values of the coupling constant are reported. FT-IR spectra were recorded on a Perkin-Elmer 681 spectrometer. GC analyses were performed by using an HP1 column (methyl siloxane; 30 m  $\times$  0.32 mm  $\times$  0.25  $\mu$ m film thickness) on a HP 6890 model, Series II. Thin-layer chromatography (TLC) was performed on silica gel sheets with fluorescent indicator, the spots on the TLC were observed under ultraviolet light or were visualized by I<sub>2</sub> vapor. Column chromatography was conducted by using Sorbent silica gel standard grade, porosity 60 Å, particle size 32–63  $\mu$ m (230  $\times$  450 mesh), surface area 500–600 m<sup>2</sup>/g, bulk density 0.4 g/mL, pH range 6.5–7.5. GC–Mass Spectrometric analyses were performed on an HP 5995C model. MS-ESI analyses were performed on Agilent 1100 LC/MSD trap system VL or on a Thermo Electron Surveyor pump and autosampler operated in-line with a Quantum triple quadrupole instrument in ESI positive or negative ion mode. Elemental analyses were performed on an Elemental Analyzer 1106-Carlo Erba-instrument.

### 4.1.1. Materials

Tetrahydrofuran (THF) from commercial source was purified by distillation (twice) from sodium wire under nitrogen. Dichloromethane and DMF from commercial source were purified by distillation from CaH<sub>2</sub> under nitrogen atmosphere. Standardized (2.5 M) *n*-butyllithium in hexanes was purchased from Aldrich Chemical Co. and its titration was performed with *N*-pivaloyl-*o*-toluidine [29]. Triethylamine from commercial source was purified by distillation from CaH<sub>2</sub> under reduced pressure and nitrogen atmosphere. All other chemicals and solvents were commercial grade further purified by distillation or crystallization prior to use. Arylnitrile oxides were prepared from aldehydes through their conversion into the corresponding oximes and then into benzo-hydroximinoyl chlorides [21,23]. These were finally converted into nitrile oxides, just before use, by treatment with NEt<sub>3</sub> at 0 °C followed by *vacuum* filtration to remove the NEt<sub>3</sub>·HCl from the THF solution. Oximes, prepared from reaction of aldehydes/EtOH and NH<sub>2</sub>OH·HCl/aq. NaOH, had analytical and spectroscopic data identical to those previously reported or commercially available [30–34].

### 4.1.2. Synthesis of 5-(bromomethyl)-3-(5-chlorofuran-2-yl)-4-phenylisoxazole (Br-P6)

To a solution of 3-(5-chloro-2-furyl)-4-phenyl-5-methylisoxazole (P6) (0.500 g, 1.930 mmol) in anhydrous CCl<sub>4</sub> (10 mL), contained in an argon-flushed, three necked flask equipped with a magnetic stirrer, an argon inlet and two dropping funnels *N*-bromosuccinimide (412 mg, 2.32 mmol) were added. Then AIBN (0.158 g, 0.965 mmol) was added, and the obtained suspension was stirred overnight at room temperature. The reaction mixture was kept under reflux for 4 h, and then water was added. The two phases, formed by adding ethyl acetate, were separated and aqueous layer was extracted three times with ethyl acetate. The combined organic extracts washed first with brine and then with 1 M KOH, were dried over anhydrous Na<sub>2</sub>SO<sub>4</sub>. The solvent was evaporated under reduced pressure. Column chromatography (silica gel, petroleum ether/ethyl acetate = 10:1) of the residue affords the 5-(bromomethyl)-3-(5-chlorofuran-2-yl)-4-phenylisoxazole in 95% yield as a solid.

### 4.1.3. 5-(Bromomethyl)-3-(5-chlorofuran-2-yl)-4-phenylisoxazole (Br-P6)

White solid (95%). FT-IR (neat): 3132, 3053, 2921, 1636, 1517, 1432, 1412, 1372, 1359, 1226, 1127, 1048, 1018, 985, 939, 903, 790, 777, 704 cm<sup>-1</sup>. <sup>1</sup>H NMR (400 MHz, CDCl<sub>3</sub>,  $\delta$ ): 7.50–7.46 (m, 3H, aromatic protons); 7.39–7.36 (m, 2H, aromatic protons); 6.31 (d,  $J = 3.5$  Hz, 1H, furyl proton); 6.15 (d,  $J = 3.5$  Hz, 1H, furyl proton); 4.38 (s, 2H, CH<sub>2</sub>). <sup>13</sup>C NMR (100 MHz, CDCl<sub>3</sub>,  $\delta$ ): 170.3, 163.5, 152.7, 143.1, 139.0, 130.2, 129.2, 129.1, 128.1, 118.1, 114.4, 108.2, 55.4, 20.7. GC–MS (70 eV)  $m/z$  (rel. int.): 341 [M (<sup>81</sup>Br, <sup>37</sup>Cl)<sup>+</sup>, 26], 339 [M (<sup>79</sup>Br, <sup>37</sup>Cl)<sup>+</sup>, 100], 337 [M (<sup>79</sup>Br, <sup>35</sup>Cl)<sup>+</sup>, 78], 258 (22), 246 (11), 244 (33), 232 (12), 230 (35), 223 (14), 219 (17), 218 (13), 217 (54), 216 (19), 190 (16), 188 (46), 167 (25), 166 (16), 163 (12), 154 (18), 153 (29), 152 (28), 140 (10), 139 (18), 129 (66), 128 (11), 127 (24), 115 (34), 103 (19), 102 (13), 91 (28), 89 (38), 77 (18), 75 (13), 73 (17), 63 (12), 51 (9). Anal. Calc. for C<sub>16</sub>H<sub>12</sub>ClNO<sub>3</sub>: C, 64.48; H, 3.81; N, 4.41. Found: C, 64.46; H, 3.82; N, 4.46.

### 4.1.4. Synthesis of 5-(fluoromethyl)-3-(5-chlorofuran-2-yl)-4-phenylisoxazole (<sup>19</sup>F-P6)

To an anhydrous 1 M solution of TBAF in THF (0.940 mL) kept under stirring in a round bottom flask at room temperature, 5-(bromomethyl)-3-(5-chlorofuran-2-yl)-4-phenylisoxazole (0.117 g, 0.350 mmol) was added. After 24 h, the reaction mixture was filtered over celite, and the solvent evaporated under reduced pressure. Column chromatography (silica gel, petroleum ether/

ethyl acetate = 8:2) of the residue affords 0.063 g of 5-(fluoromethyl)-3-(5-chlorofuran-2-yl)-4-phenylisoxazole in 65% yield as a yellow solid.

#### 4.1.5. 5-(Fluoromethyl)-3-(5-chlorofuran-2-yl)-4-phenylisoxazole (**<sup>19</sup>F-P6**)

Yellow solid (65%). Mp 82.9–84.6 °C. FT-IR (neat): 3143, 3059, 2963, 2925, 2853, 1606, 1518, 1447, 1414, 1372, 1261, 1206, 1130, 1093, 1018, 930, 899, 797, 700 cm<sup>-1</sup>. <sup>1</sup>H NMR (400 MHz, CDCl<sub>3</sub>, δ): 7.50–7.46 (m, 3H, aromatic protons); 7.39–7.35 (m, 2H, aromatic protons); 6.37 (d, *J* = 3.7 Hz, 1H, furyl proton); 6.18 (d, *J* = 3.7 Hz, 1H, furyl proton); 5.31 (d, 2H, *J* = 48 Hz, CH<sub>2</sub>). <sup>13</sup>C NMR (100 MHz, CDCl<sub>3</sub>, δ): 162.9 (d, <sup>2</sup>*J*<sub>C-F</sub> = 16.8 Hz), 152.4 (d, <sup>4</sup>*J*<sub>C-F</sub> = 3.8 Hz), 142.7, 138.9, 129.9, 129.1, 128.9, 127.5, 119.4 (d, <sup>3</sup>*J*<sub>C-F</sub> = 5.3 Hz), 114.3, 108.0, 72.2 (d, <sup>1</sup>*J*<sub>C-F</sub> = 169.4 Hz). <sup>19</sup>F NMR (376 MHz, CDCl<sub>3</sub>, δ): -146.7 (t, *J* = 48 Hz). GC-MS (70 eV) *m/z* (rel. int.): 279 [M (<sup>37</sup>Cl)<sup>+</sup>, 35], 277 [M (<sup>35</sup>Cl)<sup>+</sup>, 100], 246 (8), 244 (23), 218 (9), 216 (26), 190 (22), 188 (67), 153 (31), 152 (28), 129 (62), 128 (10), 127 (17), 89 (28), 77 (10), 73 (9), 63 (10). Anal. Calc. for C<sub>14</sub>H<sub>9</sub>ClFNO<sub>2</sub>: C, 60.56; H, 3.27; N, 5.04. Found: C, 60.46; H, 3.82; N, 4.46.

#### 4.1.6. Synthesis of [3-(5-chlorofuran-2-yl)-4-phenylisoxazol-5-yl]methyl-4-methylbenzenesulfonate (**OTs-P6**)

Triethylamine (0.8 mL, 5.854 mmol) and *p*-toluenesulfonic anhydride (954 mg, 2.926 mmol) were added to a solution of compound **HO-P6** [23,25] (236 mg, 0.858 mmol) in CH<sub>2</sub>Cl<sub>2</sub> (20 mL) at 0 °C contained in a round bottom flask equipped with a magnetic stirrer. After 2.5 h the reaction was stopped by adding H<sub>2</sub>O (10 mL) and the two phases were separated. The aqueous layer was washed three times with EtOAc. The combined organic extracts were dried over anhydrous Na<sub>2</sub>SO<sub>4</sub> and the solvent was removed under reduced pressure. Column chromatography (silica gel, mobile phase: petroleum ether/ethyl acetate = 8:2) of the residue (370 mg) afforded the product as a white solid (256 mg, 70% yield).

#### 4.1.7. [3-(5-Chlorofuran-2-yl)-4-phenylisoxazol-5-yl]methyl-4-methylbenzenesulfonate (**OTs-P6**)

White solid (70%). <sup>1</sup>H NMR (600 MHz, DMSO-*d*<sub>6</sub>, δ): 7.67–7.66 (m, 2H, aromatic protons); 7.44–7.40 (m, 5H, aromatic protons); 7.24–7.23 (m, 2H, aromatic protons); 6.59 (d, *J* = 3.4 Hz, 1H, furyl proton); 6.44 (d, *J* = 3.4 Hz, 1H, furyl proton); 5.12 (s, 2H, CH<sub>2</sub>OTs); 2.4 (s, 3H, CH<sub>3</sub>). <sup>13</sup>C NMR (600 MHz, DMSO-*d*<sub>6</sub>, δ): 161.8, 152.4, 145.9, 142.5, 137.9, 131.8, 130.7, 130.0, 129.5, 129.3, 128.1, 127.1; 115.2; 109.5; 60.5; 21.5.

#### 4.2. Radiomimetic synthesis of the [**<sup>19</sup>F**]-P6

A solution of KF (7.8 mg) in 400 μL of water was added to a mixture of 29 mg Kryptofix 2.2.2 in 1.5 mL of acetonitrile and K<sub>2</sub>CO<sub>3</sub> 1 M (29 μL). The reaction mixture was stirred for 5 min at room temperature. The solvents were evaporated using a stream of argon for 10 min at 85 °C and co-evaporated to dryness with CH<sub>3</sub>CN (400 μL for two times) and the solution was stirred at room temperature under a stream of argon for another 20 min at 85 °C to remove the residual traces of water. To the dried KF/Kryptofix complex, a solution of 8 mg of the tosylate precursor **OTs-P6** in DMSO (2 mL) was added. The reaction mixture was allowed to react at 150 °C for 20 min and subsequently cooled to room temperature. The reaction mixture was diluted with 5 mL of water and extracted with ethyl acetate (three times). Organic phases were washed with water for three times and then dried over anhydrous Na<sub>2</sub>SO<sub>4</sub>; the solvent was removed under reduced pressure. Column chromatography (silica gel, mobile phase: hexane/ethyl acetate = 8:2) afforded the product in 50% yield.

#### 4.2.1. Synthesis of [**<sup>18</sup>F**]-P6 radiotracer

The <sup>18</sup>F-radiosynthesis [27] was performed on a commercially available GE Tracerlab FX<sub>FN</sub> automated reaction module. The <sup>18</sup>F-fluoride anion (128,020 MBq) was trapped (adsorbed) onto an anion (K<sub>2</sub>CO<sub>3</sub> contained) exchange resin (QMA-cartridge) and eluted with a solution of Kryptofix 2.2.2 (12.5 mg) and K<sub>2</sub>CO<sub>3</sub> (7 mg) in CH<sub>3</sub>CN/H<sub>2</sub>O (1:1 v/v) (Scheme 2). The solvent was then evaporated under vacuum with a gentle stream of helium gas (32 kPa), followed by sequential additions of anhydrous acetonitrile and further azeotropic drying. Once drying was complete, a solution of tosylate precursor **OTs-P6** (4.4 mg) in anhydrous DMSO (0.5 mL) was added to the K<sup>18</sup>F/Kryptofix 2.2.2 complex. The reaction vessel was then sealed and the reaction mixture was heated with stirring to 140 °C for a period of 10 min. Purification of the crude product was accomplished by using semi-prep HPLC (Macherey–Nagel Nucleosil 100-7 C-18 VarioPrep Column 250 × 16 mm, EtOH/Water 60:40, flow rate 6 mL/min, *R*<sub>f</sub> 12.8 min). The [**<sup>18</sup>F**]-P6 compound peak was collected and diluted with deionized-H<sub>2</sub>O (100 mL) followed by trapping on a C-18 Sep-Pak. The final radiolabeled product [**<sup>18</sup>F**]-P6 was then eluted off of the Sep-Pak directly into the final vial using ethanol (200 proof) followed by saline (0.9%) (1:9 v/v, 10 mL), product 11,803 MBq (non-decay corrected), radiochemical yield 18% (decay corrected), radiochemical purity 95% (by radio-HPLC), Specific activity: 176,305 MBq/mmol. A radio-HPLC chromatogram of a typical radiosynthesis is shown in Fig. 5.

#### 4.3. Biology

##### 4.3.1. Human ovarian cancer cell (OVCAR 3) viability assay

Human adenocarcinoma cells NIH:OVCAR-3 (HTB-161) (ATCC, passage number 8–20, mycoplasma-negative by pcr mycoplasma detection assay) were grown at 37 °C in a humidified incubator

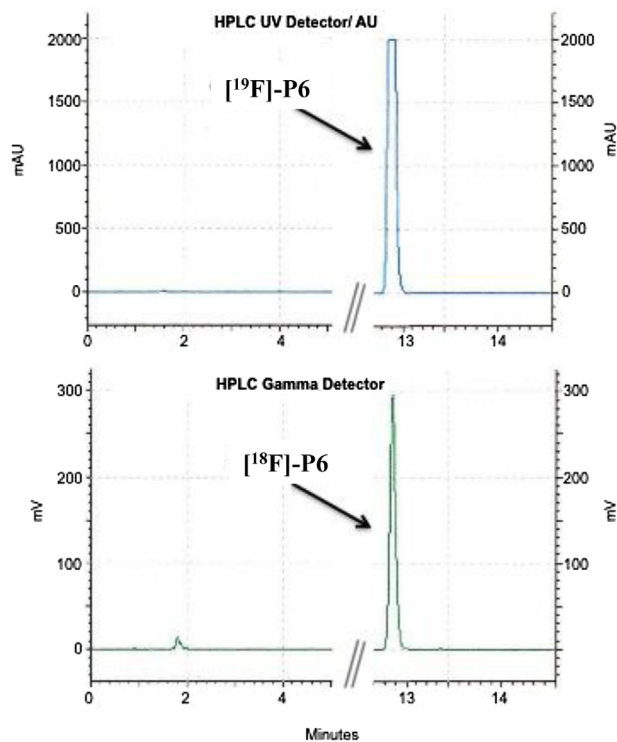


Fig. 5. HPLC chromatogram of [**<sup>18</sup>F**]-P6 compared with cold standard [**<sup>19</sup>F**]-P6 (*R*<sub>f</sub> = 12.8 min). The HPLC analysis was performed using Macherey–Nagel Nucleosil 100-7 C-18 VarioPrep Column 250 × 16 mm, mobile phase EtOH/Water = 60:40 and flow rate = 6 mL/min.

with 5% CO<sub>2</sub> in RPMI 1640 + 10% FBS. Cells were plated in growth medium at 7000–8000 cells per well (100 µL) in 96 well plates (Sarstedt) and allowed to attach for 24 h. No cells were plated in the first column. Fresh RPMI 1640 + 10% FBS + penicillin/streptomycin (100 µL) containing the final concentrations of DMSO or test compound dilutions in DMSO (DMSO final concentration, 0.1%) was replaced in each well. After 48 h of cell growth with respective treatments, WST-1 Cell Proliferation Reagent (Roche, 11644807001) was added (10 µL) to each well, then the plate was incubated for 45–60 min at 37 °C. The formazan crystals were solubilized using 100 µL of DMSO and the absorbance values were read (Molecular Devices) at 450 nm. Six replicates were used in the calculations per treatment concentration in duplicate experiments.

#### 4.3.2. [<sup>14</sup>C]-Arachidonic acid TLC COX activity assay by using purified oCOX-1 and mCOX-2 enzymes

COX inhibition screening assay to evaluate compounds as competitive inhibitors: time- and concentration-dependent inhibition reactions were performed by pre-incubating inhibitor and hematin-reconstituted enzyme in 100 mM Tris–HCl buffer with 500 µM phenol for 17 min at room temperature followed by a 3 min incubation at 37 °C. Following the addition of 5 µM [<sup>14</sup>C]-AA (~Km of arachidonate), samples were incubated for 30 s at 37 °C, and the reactions were then terminated by extraction with diethyl ether/methanol/citrate (30:4:1). The extracts were analyzed for substrate consumption by thin-layer chromatography as previously described [35]. All inhibitor concentrations for 50% enzyme activity (IC<sub>50</sub>) were determined by nonlinear regression analysis using Graphpad Prism software and were the average of at least two independent experiments. All inhibitors were prepared as stock solutions in dimethylsulfoxide (DMSO), and diluted into reaction buffer so that the final DMSO concentration was 2.5% in all samples. Reactions were run with hematin-reconstituted proteins at final enzyme concentrations adjusted to give approximately 30% substrate consumption. AA was prepared as a stock solution in 0.1 N NaOH.

#### 4.3.3. In vitro OVCAR-3 cell assay

Human ovarian adenocarcinoma cells, OVCAR 3, passage 13–17, mycoplasma negative by PCR detection method (Sigma VenorGem) were grown in RPMI 1640 (Invitrogen/Gibco) + 10% FBS (Atlas) to 70% confluence. Cells were plated in 6-well plates (Sarstedt) and grown to ~60% confluency. Warm HBSS/Tyrodes 1:1 (2 mL) was replaced in each well, and the cells were treated with inhibitor dissolved in DMSO (0.2–50 µM, final concentration) for 30 min at 37 °C followed by the addition of [<sup>14</sup>C]-arachidonic acid [8 µM, ~2035 MBq/mmol, Perkin Elmer] for 30 min at 37 °C. Aliquots (400 µL) were removed and the reactions were terminated by solvent extraction in 400 µL ice-cold Et<sub>2</sub>O/CH<sub>3</sub>OH/1 M citrate, pH 4.0 (30:4:1). The organic phase was spotted on a 20 × 20 cm TLC plate (EMD Kieselgel 60, VWR). The plate was developed in EtOAc/CH<sub>2</sub>Cl<sub>2</sub>/glacial AcOH (75:25:1), and radiolabeled prostaglandins were quantified with a radioactivity scanner (Bioscan, Inc., Washington, D.C.). The percentage of total products observed at different inhibitor concentrations was divided by the percentage of products observed for cells pre-incubated with DMSO.

#### 4.4. In vivo stability of compound [<sup>19</sup>F]-P6 and its tumor vs normal leg muscle distribution

Animal studies were conducted in accordance with the standards of humane animal care described in the NIH Guide for the Care and Use of Laboratory Animals, using protocols approved by the Vanderbilt University institutional animal care and use committee. Animals were housed in an Association for the Assessment

and Accreditation of Laboratory Animal Care (AAALAC)-approved animal care facility.

*In vivo* stability of compound [<sup>19</sup>F]-P6 was evaluated by analyzing the tissue samples on an LC–ESI-MS system. A group of four animals (nude mice) were injected with Human Ovarian Cancer 3 (OVCAR 3) cells on the left flank subcutaneously. The tumor xenografts were allowed to grow to approximately 750 mm<sup>3</sup> for 2 months. The nude mice bearing OVCAR-3 xenografts were dosed with intraperitoneal (i.p.) injection of [<sup>19</sup>F]-P6 (2 mg/kg) dissolved in dimethylsulfoxide (DMSO). Surgery was performed to collect tumors and normal leg muscles. The tissue samples were weighed, and snap-frozen at –80 °C for storage. For analysis, the frozen tissue was thawed and digested with Proteinase K (Sigma) overnight. An aliquot of the digestion solution was extracted with 1.2 volumes of EtOAc/*n*-Hexane (2:1). The organic layer was removed, dried and reconstituted in MeOH and water. The unknown samples were quantitated against a 5-point standard curve, which was subjected to the Proteinase K digestion and liquid–liquid extraction. The compounds were separated in reverse-phase mode on a C<sub>18</sub> column (5 × 0.2 cm, Phenomenex) using gradient elution. Mobile phase component A was water and B was acetonitrile, each with 0.1% acetic acid. The gradient used was 50% B to 80% B over 4 min, followed by a brief hold and return to initial conditions. The flow rate was 0.30 mL/min. The samples were analyzed on an LC–ESI-MS system (Thermo) and compound [<sup>19</sup>F]-P6 was detected via selected reaction monitoring. The intact parent compound [<sup>19</sup>F]-P6 was identified in the tumors on an average of 63 pmol/g tissue (*n* = 4) (Fig. 4). A minimal or no amount of the compound [<sup>19</sup>F]-P6 was detected in the normal leg muscles. Also, no defluorinated metabolite (compound HO-P6) was detected in any of the tissue samples analyzed, suggesting that compound [<sup>19</sup>F]-P6 remained intact in the biological environment for long enough period of time to be taken up by the COX-1-expressing tumors (Fig. 4).

#### 4.5. In vivo PET-CT investigation by [<sup>18</sup>F]-P6

We evaluated the ability of [<sup>18</sup>F]-P6 to target COX-1 in human ovarian tumor xenografts (Fig. 2). Female nude mice, NU-Fox1nu, were purchased at 6–7 weeks of age from Charles River Labs. Human OVCAR-3 cells were trypsinized and resuspended in cold PBS containing 30% Matrigel such that 1 × 10<sup>6</sup> cells in 100 µL were injected subcutaneously on the left flank. The tumor xenografts were allowed to grow to approximately 750 mm<sup>3</sup>. The OVCAR-3 xenografts required 2–3 months of growth. Mice bearing OVCAR-3 xenografts were dosed with intraperitoneal injection with [<sup>18</sup>F]-P6 (100 µL, 7.4 MBq), formulated in dimethylsulfoxide (10%), ethanol (40%) and sterile saline (50%). Four hours post-injection, the animals were anesthetized with 2% isoflurane and positioned in the microPET Focus 220 (Siemens), and 30 min acquisition (24 projections × 60 s per projection) was started. CT images of the hips were then produced by the microCAT II (Siemens, Knoxville, TN) at X-ray beam intensity of 500 mA and tube voltage of 80 kVp. The PET images were reconstructed using an OSEM3D/MAP algorithm into transaxial slices (128 × 128 × 95) with voxel sizes of 0.095 cm × 0.095 cm × 0.08 cm. The PET and CT images were co-registered to each other on the basis of bed position. After imaging, the mice were sacrificed by isoflurane overdose. The OVCAR 3 tumors were removed and weighed, and radioactivity associated with each tumor was counted with a well gamma counter. After normalization of uptake (Bq/g), the OVCAR 3 tumors showed approximately an 8-fold higher uptake of the radiotracer compared with normal leg muscle as shown in Fig. 2 (*n* = 3, *p* = 0.01).

## Acknowledgment

This work has been supported by a grant from the National Institutes of Health, USA (CA128323) and Ministero dell'Istruzione dell'Università e della Ricerca (Italy, PRIN 20097FJHPZ\_001), and a graduate scholarship to PM from University of Bari (Italy). Authors are grateful to Mr. Donel of the Department of Radiology and Radiological Sciences for radio-HPLC analysis optimization condition assistance.

## References

- [1] A.L. Blobaum, L.J. Marnett, Structural and functional basis of cyclooxygenase inhibition, *Journal of Medicinal Chemistry* 50 (2007) 1425–1441.
- [2] M.G. Perrone, A. Scilimati, L. Simone, P. Vitale, Selective COX-1 inhibition: a therapeutic target to be reconsidered, *Current Medicinal Chemistry* 17 (2010) 3769–3805.
- [3] Z.A. Radi, N.K. Khan, Effect of cyclooxygenase inhibition on the gastrointestinal tract, *Experimental and Toxicologic Pathology* 58 (2006) 163–173.
- [4] G. Li, T. Yang, J. Yan, Cyclooxygenase-2 increased the angiogenic and metastatic potential of tumor cells, *Biochemical and Biophysical Research Communications* 299 (2002) 886–890.
- [5] S.-H. Choi, S. Aid, F. Bosetti, The distinct roles of cyclooxygenase-1 and -2 in neuroinflammation: implications for translational research, *Trends in Pharmacological Sciences* 30 (2009) 174–181.
- [6] R. Calvello, M.A. Panaro, M.L. Carbone, A. Cianciulli, M.G. Perrone, P. Vitale, P. Malerba, A. Scilimati, Novel selective COX-1 inhibitors suppress neuro-inflammatory mediators in LPS-stimulated N13 microglial cells, *Pharmacological Research* 66 (2012) 137–148.
- [7] V. Evangelista, S. Manarini, A. Di Santo, M.L. Capone, E. Ricciotti, L. Di Francesco, S. Tacconelli, A. Sacchetti, S. D'Angelo, A. Scilimati, M.G. Sciuilli, P. Patrignani, De novo synthesis of cyclooxygenase-1 counteracts the suppression of platelet thromboxane biosynthesis by aspirin, *Circulation Research* 98 (2006) 593–595.
- [8] A. Virdis, R. Colucci, M. Fornai, E. Duranti, C. Giannarelli, N. Bernardini, C. Segnani, C. Ippolito, L. Antonioli, C. Blandizzi, S. Taddei, A. Salvetti, M. Del Tacca, Cyclooxygenase-1 is involved in endothelial dysfunction of mesenteric small arteries from infused mice, *Hypertension* 49 (2007) 679–686.
- [9] J. Cao, T. Kitazawa, K. Takehana, T. Taneike, Endogenous prostaglandins regulate spontaneous contractile activity of uterine strips isolated from non-pregnant pigs, *Prostaglandins & Other Lipid Mediators* 81 (2006) 93–105.
- [10] X. Zhu, D. Conklin, J.C. Eisenach, Cyclooxygenase-1 in the spinal cord plays an important role in postoperative pain, *Pain* 104 (2003) 15–23.
- [11] A. Kirschenbaum, A.P. Klausner, P. Le, P. Unger, S. Yao, X.-H. Liu, A.C. Levine, Expression of cyclooxygenase-1 and cyclooxygenase-2 in the human prostate, *Urology* 56 (2000) 671–676.
- [12] D. Hwang, D. Scollard, J. Byrne, E. Levine, Expression of cyclooxygenase-1 and cyclooxygenase-2 in human breast cancer, *Journal of the National Cancer Institute* 90 (1998) 455–460.
- [13] T. Daikoku, S. Tranguch, I.N. Trofimova, D.M. Dinulescu, T. Jacks, A.Y. Nikitin, D.C. Connolly, S.K. Dey, Cyclooxygenase-1 is overexpressed in multiple genetically engineered mouse models of epithelial ovarian cancer, *Cancer Research* 66 (2006) 2527–2531.
- [14] B.M. Erovic, M. Woegerbauer, J. Pammer, E. Selzer, M.C. Grasl, D. Thurnher, Strong evidence for up-regulation of cyclooxygenase-1 in head and neck cancer, *European Journal of Clinical Investigation* 38 (2007) 61–66.
- [15] M. Li, R. Lotan, B. Levin, E. Tahara, S.M. Lippman, X.-C. Xu, Aspirin induction of apoptosis in esophageal cancer: a potential for chemoprevention, *Cancer Epidemiology, Biomarkers & Prevention* 9 (2000) 545–549.
- [16] R.A. Gupta, L.V. Tejada, B.J. Tong, S.K. Das, J.D. Morrow, S.K. Dey, R.N. DuBois, Cyclooxygenase-1 is overexpressed and promotes angiogenic growth factor production in ovarian cancer, *Cancer Research* 63 (2003) 906–911.
- [17] T. Daikoku, D. Wang, S. Tranguch, J.D. Morrow, S. Orsulic, R.N. DuBois, S.K. Dey, Cyclooxygenase-1 is a potential target for the prevention and treatment of ovarian epithelial cancer, *Cancer Research* 65 (2005) 3735–3744.
- [18] W. Li, Z.-L. Ji, G.-C. Zhuo, R.-J. Xu, J. Wang, H.-R. Jiang, Effects of a selective cyclooxygenase-1 inhibitor in SKOV-3 ovarian carcinoma xenograft-bearing mice, *Medical Oncology* 27 (2010) 98–104.
- [19] W. Li, R.J. Xu, Z.Y. Lin, G.C. Zhuo, H.H. Zhang, Effects of a cyclooxygenase-1 selective inhibitor in a mouse model of ovarian cancer, administered alone or in combination with ibuprofen, a nonselective cyclooxygenase inhibitor, *Medical Oncology* 26 (2009) 170–177.
- [20] C.M. Telleria, Repopulation of ovarian cancer cells after chemotherapy, *Cancer Growth and Metastasis* 6 (2013) 15–21.
- [21] L. Di Nunno, P. Vitale, A. Scilimati, S. Tacconelli, P. Patrignani, Novel synthesis of 3,4-diarylisoxazole analogues of valdecoxib: reversal COX-2 selectivity by sulfonamide group removal, *Journal of Medicinal Chemistry* 47 (2004) 4881–4890.
- [22] M.G. Perrone, P. Vitale, P. Malerba, A. Altomare, R. Rizzi, A. Lavecchia, C. Di Giovanni, E. Novellino, A. Scilimati, Diarylheterocycle core ring features effect in selective COX-1 inhibition, *ChemMedChem* 7 (2012) 629–641.
- [23] P. Vitale, S. Tacconelli, M.G. Perrone, P. Malerba, L. Simone, A. Scilimati, A. Lavecchia, M. Dovizio, M. Marcantoni, A. Bruno, P. Patrignani, Synthesis, pharmacological characterization and docking analysis of a novel family of diarylisoxazoles as highly selective COX-1 inhibitors, *Journal of Medicinal Chemistry* 56 (2013) 4277–4299.
- [24] P. Vitale, M.G. Perrone, P. Malerba, A. Lavecchia, A. Scilimati, Selective COX-1 inhibition as a target of theranostic novel diarylisoxazoles, *European Journal of Medicinal Chemistry* 74 (2014) 606–618.
- [25] A. Scilimati, P. Vitale, L. Di Nunno, P. Patrignani, S. Tacconelli, M.L. Capone, Patent US 2011, 7,989,450 B2.
- [26] A. Scilimati, L. Di Nunno, P. Vitale, S. Tacconelli, P. Patrignani, S. Tacconelli, E. Porreca, L. Stuppia, Isoxazole Derivatives and Their Use as Cyclooxygenase Inhibitors, PCT Int. 2005, WO2005068442.
- [27] M.J. Uddin, B.C. Crews, K. Ghebreselasie, I. Huda, P.J. Kingsley, M.S. Ansari, M.N. Tantawy, J. Reese, L.J. Marnett, Fluorinated COX-2 inhibitors as agents in PET imaging of inflammation and cancer, *Cancer Prevention Research* 4 (2011) 1536–1545.
- [28] A.S. Kalgutkar, A.B. Marnett, B.C. Crews, R.P. Remmel, L.J. Marnett, Ester and amide derivatives of the nonsteroidal anti-inflammatory drug, indomethacin, as selective cyclooxygenase-2 inhibitors, *Journal of Medicinal Chemistry* 43 (2000) 2860–2870.
- [29] J. Suffert, Simple direct titration of organolithium reagents using N-pivaloyl-o-toluidine and/or N-pivaloyl-o-benzylaniline, *Journal of Organic Chemistry* 54 (1989) 509–510.
- [30] L. Di Nunno, P. Vitale, A. Scilimati, Effect of the aryl group substituent in the dimerization of 3-arylisoxazoles to syn 2,6-diaryl-3,7-diazatricyclo [4.2.0.0<sup>2,5</sup>]octan-4,8-diones induced by LDA, *Tetrahedron* 64 (2008) 11198–11204.
- [31] L. Di Nunno, P. Vitale, A. Scilimati, L. Simone, F. Capitelli, Stereoselective dimerization of 3-arylisoxazoles to cage-shaped bis-β-lactams syn-2,6-diaryl-3,7-diazatricyclo [4.2.0.0<sup>2,5</sup>]octan-4,8-diones induced by hindered lithium amides, *Tetrahedron* 63 (2007) 12388–12395.
- [32] L. Di Nunno, A. Scilimati, Synthesis of 3-aryl-4, 5-dihydro-5-hydroxy-1,2-oxazoles by reaction of substituted benzonitrile oxides with the enolate ion of acetaldehyde, *Tetrahedron* 43 (1987) 2181–2189.
- [33] L. Di Nunno, A. Scilimati, P. Vitale, 5-Hydroxy-3-phenyl-5-vinyl-2-isoxazoline and 3-phenyl-5-vinylisoxazole: synthesis and reactivity, *Tetrahedron* 61 (2005) 11270–11278.
- [34] P. Vitale, L. Di Nunno, A. Scilimati, A novel synthesis of N-unsubstituted β-enamino thioesters from 3-arylisoxazoles and 3-aryl-5-phenylthio-2-isoxazolines, *Synthesis* 18 (2010) 3195–3203.
- [35] A.S. Kalgutkar, B.C. Crews, S.W. Rowlinson, C. Garner, K. Seibert, L.J. Marnett, Aspirin-like molecules that covalently inactivate cyclooxygenase-2, *Science (Washington, D.C.)* 280 (1998) 1268–1270.